

Manipulation of nonreciprocal unconventional photon blockade in a cavity-driven system composed of an asymmetrical cavity and two atoms with weak dipole-dipole interaction

Xinqin Zhang(张新琴), Xiuwen Xia(夏秀文), Jingping Xu(许静平), Haozhen Li(李浩珍), Zeyun Fu(傅泽云), and Yaping Yang(羊亚平)

Citation: Chin. Phys. B, 2022, 31 (**7**): 074204. DOI: 10.1088/1674-1056/ac523f
Journal homepage: http://cpb.iphy.ac.cn; http://iopscience.iop.org/cpb

What follows is a list of articles you may be interested in

Improved dielectric and electro-optical parameters of nematic liquid crystal doped with magnetic nanoparticles

Geeta Yadav, Govind Pathak, Kaushlendra Agrahari, Mahendra Kumar, Mohd Sajid Khan, V S Chandel, Rajiv Manohar
Chin. Phys. B, 2019, 28 (**3**): 034209. DOI: 10.1088/1674-1056/28/3/034209

A sensitive detection of high Rydberg atom with large dipole moment

Shan-Shan Zhang(张珊珊), Hong Cheng(成红), Pei-Pei Xin(辛培培), Han-Mu Wang(王汉睦), Zi-Shan Xu(徐子珊), Hong-Ping Liu(刘红平)
Chin. Phys. B, 2018, 27 (**7**): 074207. DOI: 10.1088/1674-1056/27/7/074207

Photon bunching and anti-bunching with two dipole-coupled atoms in an optical cavity

Ya-Mei Zheng(郑雅梅), Chang-Sheng Hu(胡长生), Zhen-Biao Yang(杨贞标), Huai-Zhi Wu(吴怀志)
Chin. Phys. B, 2016, 25 (**10**): 104202. DOI: 10.1088/1674-1056/25/10/104202

Position-dependent property of resonant dipole—dipole interaction mediated by localized surface plasmon of an Ag nanosphere

Xu Dan, Wang Xiao-Yun, Huang Yong-Gang, Ouyang Shi-Liang, He Hai-Long, He Hao
Chin. Phys. B, 2015, 24 (**2**): 024205. DOI: 10.1088/1674-1056/24/2/024205

Measurement-induced disturbance between two atoms in Tavis–Cummings model with dipole–dipole interaction

Zhang Guo-Feng, Wang Xiao, Lü Guang-Hong
Chin. Phys. B, 2014, 23 (**10**): 104204. DOI: 10.1088/1674-1056/23/10/104204

Manipulation of nonreciprocal unconventional photon blockade in a cavity-driven system composed of an asymmetrical cavity and two atoms with weak dipole–dipole interaction

Xinqin Zhang(张新琴)[1], Xiuwen Xia(夏秀文)[1,2,†], Jingping Xu(许静平)[2], Haozhen Li(李浩珍)[3], Zeyun Fu(傅泽云)[1], and Yaping Yang(羊亚平)[2]

[1] *Institute of Atomic and Molecular Physics and Functional Materials, School of Mathematics and Physics, Jinggangshan University, Ji'an* 343009, *China*

[2] *MOE Key Laboratory of Advanced Micro-structure Materials, School of Physics Science and Engineering, Tongji University, Shanghai* 200092, *China*

[3] *College of Communication Engineering, Hangzhou Dianzi University, Hangzhou* 310018, *China*

(Received 9 December 2021; revised manuscript received 24 January 2022; accepted manuscript online 7 February 2022)

We present a work of manipulating collective unconventional photon blockade (UCPB) and nonreciprocal UCPB (NUCPB) in a cavity-driven system composed of an asymmetrical single-mode cavity and two interacting identical two-level atoms (TLAs). When the atoms do not interact directly, the frequency and intensity restrictions of collective UCPB can be specified, and a giant NUCPB exists due to the splitting of optimal atom–cavity coupling strength in proper parameter regime. However, if a weak atom–atom interaction which provides a new and feeble quantum interference pathway to UCPB is taken into account, two restrictions of UCPB are combined complexly, which are rigorous to be matched simultaneously. Due to the push-and-pull effect induced by weak dipole–dipole interaction, the UCPB regime is compressed more or less. NUCPB is improved as a higher contrast is present when the two complex UCPB restrictions are matched, while it is suppressed when the restrictions are mismatched. In general, whether NUCPB is suppressed or promoted depends on its working parameters. Our findings show a prospective access to produce giant quantum nonreciprocity by a couple of weakly interacting atoms.

Keywords: unconventional photon blockade, quantum nonreciprocity, dipole–dipole interaction

PACS: 42.50.Pq, 42.50.Gy **DOI:** 10.1088/1674-1056/ac523f

1. Introduction

Photon blockade (PB), especially one-photon blockade, provides an efficient way to produce antibunching photon source, which plays an important role in quantum metrology and quantum information technology. The first strong two-mode PB has been proposed in two coupled Kerr-like nonlinear coupler, in which the quantum evolution can be closed within a finite set of n-photon Fock states,[1] and has been observed in an optical cavity with one trapped atom.[2] Due to the potential applications in quantum communication and quantum networking, the study of PB has been paid extensive attention in various systems recently.[3–9]

Compared with the conventional photon blockade (CPB), which is induced by anharmonicity,[10–14] quantum destruction interference induced unconventional photon blockade (UCPB) provides a strong PB effect beyond the strong coupling limitation.[15–26] Researches have shown UCPB in both cavity- and atom-driven cavity QED system recently.[27–29] However, the collective UCPB in asymmetrical cavity with and without atom-atom interaction are not revealed.

Quantum nonreciprocity in optical region is a kind of nonclassical optical nonreciprocity. The combination of PB effect and quantum nonreciprocity is prospective in achieving back-action-free quantum sensing and chiral photonic communication, which has been proposed firstly in a high-speed spinning optomechanical system,[30] and has been explored in various systems in the consequent works.[31–37] Anti-bunching or bunching photon outcomes when the incident direction is alternated. However, the vibration disturbance of mechanical rotation is always irksome and does damage to the brittle quantum procedure. As we know, Lorentz reciprocity breaking is essential to optical nonreciprocity, which is related to the collaboration of spatial symmetry breaking, time-reversal symmetry breaking and optical nonlinearity.[38–40] In this sense, the rotating ring cavity in a certain direction plays the role of breaking spacial symmetry. Producing nonreciprocal UCPB (NUCPB) without any mechanical motion, is not only beneficial to weaken the operating difficulty, but also to improve the stability of NUCPB effect.

In this work, we will introduce an all-optical NUCPB in atom–cavity QED system composed of an asymmetrical cavity and two interacting identical two-level atoms (TLAs), where the spacial symmetry is broken naturally by asymmetrical cavity. In the atom–cavity coupling system, quantum destructive interference can lead to collective UCPB and giant NUCPB, and weak dipole–dipole interaction provides a new and feeble perturbation to quantum interference pathways.

[†]Corresponding author. E-mail: jgsuxxw@126.com

© 2022 Chinese Physical Society and IOP Publishing Ltd

The structure of this paper is organized as follows. In Section 2, the model of two identical atoms embedded in an asymmetrical cavity and the Hamiltonian are introduced and solved mathematically. In Section 3, two restrictions for UCPB are formulized. Controllable UCPB, as well as manipulation of normal and giant NUCPB are discussed in detail. The conclusions are given in Section 4.

2. Theoretical model

Recently, UCPB in cavity-driven QED with one or two identical TLAs in symmetrical cavity has been discussed, showing a prospective UCPB in weak coupling regimes.[28] Here, we adopt the concise model by considering two interacting TLAs with transition frequency $\omega_{\rm a}$ embedded in the center of a single-mode asymmetrical cavity with frequency $\omega_{\rm c}$. Different with previous works, we introduce a weak dipole–dipole interaction G between two atoms in the asymmetrical cavity. The cavity is driven by a continuous-wave (CW) coherent field with frequency $\omega_{\rm L}$, where $\delta_{\rm a}=\omega_{\rm a}-\omega_{\rm L}$ ($\delta_{\rm c}=\omega_{\rm c}-\omega_{\rm L}$) is the detuning between the atom (cavity) and input field. We respectively denote g and γ as the single-atom-cavity coupling strength and atomic spontaneous decay rate, and the non-radiation dephasing effect is ignored by letting $\gamma_{\rm non}=0$ in this work. The schematic diagram is shown in Fig. 1(a).

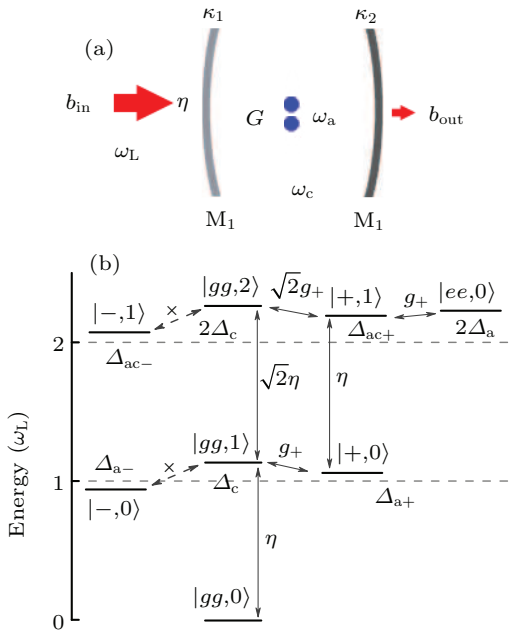


Fig. 1. (a) Scheme of the asymmetrical cavity–atoms coupling system driven by CW on the left wall M_1 with driving strength η. Here, cavity-loss rate κ_1 (κ_2) represents the decay of cavity mode through M_1 (M_2), $\omega_{\rm a}$ ($\omega_{\rm c}$ and $\omega_{\rm L}$) the frequency of atom (cavity and light), and G the atom-atom interacting strength. Panel (b) shows the transition pathways in the detuned cavity-driven case in weak driving limitation.

In order to break the spatial symmetry, cavity-loss rates κ_1 and κ_2 of the cavity walls M_1 and M_2 are different from each other in general, fulfilling $\kappa_i=-c\ln R_i/2L$ ($i=1,\,2$), where c is the velocity of light, R_i is the reflectance of cavity wall M_i, and L is the effective length of the optical cavity. The cavity is symmetrical only when $\kappa_1=\kappa_2$. We present $\kappa_{\rm ave}=(\kappa_1+\kappa_2)/2$ is the average cavity-loss rate, and the total cavity-loss rate is $\kappa=\kappa_{\rm ave}+\kappa_{\rm loss}$ where $\kappa_{\rm loss}$ represents the cavity mode dissipation. We fix $\kappa_{\rm loss}/\kappa\ll 1$ as the high-quality and low dissipation cavity is considered in this work.

In a frame rotating with the frequency of input field $\omega_{\rm L}$, the Hamiltonian of the cavity-driven system is

$$\begin{aligned}H/\hbar=&\,\Delta_{\rm a}\sum_{i=1}^{2}\sigma_i^{\dagger}\sigma_i+\Delta_{\rm c}a^{\dagger}a+g\sum_{i=1}^{2}\left(\sigma_i^{\dagger}a+a^{\dagger}\sigma_i\right)\\&+G\left(\sigma_1^{\dagger}\sigma_2+\sigma_2^{\dagger}\sigma_1\right)+H_{\rm d},\end{aligned}\tag{1}$$

where $\Delta_{\rm a}=\delta_{\rm a}-{\rm i}\gamma/2$ and $\Delta_{\rm c}=\delta_{\rm c}-{\rm i}\kappa/2$ represent the complex detunings, and $G=\frac{\mu^2}{4\pi\varepsilon_0 r^3}\left(1-3\cos^2\theta\right)$ presents a weak direct dipole–dipole interaction between two identical atoms. Here, atom–atom interaction is described by dipole–dipole coupling as the identical atoms are abstracted out as dipoles with the same electric dipole moment μ. The displacement between two atoms is r and θ is the angle between the two vectors.

The first two items are the energies of the bare atoms and cavity field, the third and fourth items, respectively, represent the atom–cavity coupling and atom–atom interaction. In quantum physics picture, weak atom–atom coupling originates from slightly overlapped wave function of two adjacent atoms. In especial, for atoms in Rydberg states, wave functions may overlap more or less when atoms are close enough. Two atoms excite each other by dexexciting itself to the ground state. $H_{\rm d}=\eta(a+a^{\dagger})$ is the cavity-driven term with η being the effective driving strength. Here, a is the annihilation operator of cavity mode, and $\sigma_i=|g\rangle_{ii}\langle e|$ ($i=1,\,2$) are the atomic pseudo spin operators.

If the external light field is incident on left wall (M_1) of the cavity and transmits through the right wall (M_2), we define it as the forward case, as shown in Fig. 1(a). Meanwhile the backward case is the opposite one, in which light propagates from M_2 to M_1. The effective driving strength $\eta=\sqrt{\kappa_i}b_{\rm in}$ ($i=1$ or 2) is relied on the driving direction, where $b_{\rm in}=\sqrt{n_{\rm in}}$ and $n_{\rm in}=\frac{P_{\rm in}}{\hbar\omega_{\rm L}}$, respectively, characterize the normalized amplitude and intensity of incoming field with power $P_{\rm in}$. We focus on UCPB in asymmetrical cavity of the forward case at first, and that of the backward case can be easily obtained by alternating κ_1 with κ_2.

It is convenient to show the physical mechanism of the coupled system by using the collective basis $|gg,n+1\rangle$, $|\pm,n\rangle=(|eg,n\rangle\pm|ge,n\rangle)/\sqrt{2}$ and $|ee,n-1\rangle$. Here, the state $|\alpha\beta,n\rangle=|\alpha\beta\rangle\otimes|n\rangle$ is the abbreviation of the atoms and cavity product state. The antisymmetric state $|-,n\rangle$ is dark since

it does not interact with other states. We truncate the Hilbert space into the two-quantum manifold which is allowed in the assumption of weak driving limitation. The wave function is reading

$$\Psi = \sum_{n=0}^{2} c_{gg,n}\left|gg,n\right\rangle + \sum_{n=0}^{1} c_{+,n}\left|+,n\right\rangle + c_{ee,0}\left|ee,0\right\rangle, \quad (2)$$

where $|c_{\alpha\beta,n}|^2$ (α, $\beta = g$, e and $n = 0$, 1, 2) is the probability of state $|\alpha\beta,n\rangle$. In the weak driving approximation, $|c_{gg,0}| \gg \{|c_{gg,1}|,|c_{+,0}|\} \gg \{|c_{+,1}|,|c_{ee,0}|\}$ and $c_{gg,0} \approx 1$ are reasonable especially in the regime of UCPB which have been adopted widely in previous works.

As mentioned in Ref. [28] and shown in Fig. 1(b), there are three interferential pathways corresponding to the transition from $|gg,1\rangle$ to $|gg,2\rangle$. One is the direct pathway of $|gg,1\rangle \leftrightarrow |gg,2\rangle$ through pumping effect, and the other is the pathway of $|gg,1\rangle \leftrightarrow |+,0\rangle \leftrightarrow |+,1\rangle \leftrightarrow |gg,2\rangle$ combined the pumping effect and atom–cavity interaction, and the third one is the pathway of $|gg,1\rangle \leftrightarrow |+,0\rangle \leftrightarrow |+,1\rangle \leftrightarrow |ee,0\rangle \leftrightarrow |+,1\rangle \leftrightarrow |gg,2\rangle$. If the three quantum channels intervene destructively and completely, the two-photon excitation will not be allowed and the probability of detecting bunching photons will be zero.

The evolution of the wave function is governed by Schrödinger equation. Following a much standard procedure which has been applied widely in previous works, the equation can be solved analytically and be simulated numerically. By setting column vectors as $C = \left(c_{gg,1}\ c_{+,0}\ c_{gg,2}\ c_{+,1}\ c_{ee,0}\right)^{\mathrm{T}}$ and $A = \left(-\eta c_{gg,0}\ 0\ 0\ 0\ 0\right)^{\mathrm{T}}$, we can get the dynamical equations for the amplitudes of each state reading

$$\mathrm{i}\,\mathrm{d}C/\mathrm{d}t = MC - A, \quad (3)$$

where the 5×5 matrix M is the truncated Hamiltonian in the two-exciton framework reading

$$M = \begin{pmatrix} \Delta_{\mathrm{c}} & g_+ & \sqrt{2}\eta & 0 & 0 \\ g_+ & \Delta_{\mathrm{a}+} & 0 & \eta & 0 \\ \sqrt{2}\eta & 0 & 2\Delta_{\mathrm{c}} & \sqrt{2}g_+ & 0 \\ 0 & \eta & \sqrt{2}g_+ & \Delta_{\mathrm{ac}+} & g_+ \\ 0 & 0 & 0 & g_+ & 2\Delta_{\mathrm{a}} \end{pmatrix}. \quad (4)$$

Here, we note $\Delta_{\mathrm{a}+} = \Delta_{\mathrm{a}} + G$, $\Delta_{\mathrm{ac}+} = \Delta_{\mathrm{a}} + \Delta_{\mathrm{c}} + G$ and $g_+ = \sqrt{2}g$. Basically, the differential group of Eq. (3) can be numerically solved by using Runge–Kutta method. Meanwhile, according to the Cramer's rule, the steady solution can be obtained approximately by setting $c_{gg,0} \equiv 1$, reading

$$C_i = D_i/D, \quad (5)$$

where C_i is the i-th component of vector C, $D = \det(M)$ and $D_i = \det(M_i)$ are the determinants of M and M_i , where M_i is the transformation of matrix M by replacing the i-th column with column vector A. Then, one can get the intensity of the cavity field $n_{\mathrm{c}} = \langle a^\dagger a\rangle$ as

$$n_{\mathrm{c}} = \left|c_{gg,1}\right|^2 + \left|c_{+,1}\right|^2 + 2\left|c_{gg,2}\right|^2. \quad (6)$$

It indicates that the cavity filed is composed of both bunching and anti-bunching components in general. By introducing the output filed operator b_{out} and applying the quantum input–output theory,[41] we can get

$$b_{\mathrm{out}} = -\mathrm{i}\sqrt{\kappa_2}a. \quad (7)$$

The outcoming field power from cavity wall M_2 is $P_{\mathrm{out}} = n_{\mathrm{out}}\hbar\omega_{\mathrm{L}}$, where $n_{\mathrm{out}} = \langle b_{\mathrm{out}}^\dagger b_{\mathrm{out}}\rangle = \kappa_2 n_{\mathrm{c}}$ is the normalized output intensity. The equal-time second-correlation function for the output photons is

$$g^{(2)}(0) = \frac{\left\langle b_{\mathrm{out}}^\dagger b_{\mathrm{out}}^\dagger b_{\mathrm{out}} b_{\mathrm{out}}\right\rangle}{\left\langle b_{\mathrm{out}}^\dagger b_{\mathrm{out}}\right\rangle^2} = 2\left|c_{gg,2}\right|^2/n_{\mathrm{c}}^2. \quad (8)$$

The antibunching light without any bunching photon can be obtained by solving either $g^{(2)}(0) = 0$ or $D_3 = 0$. Restrictions for fully antibunching output can be obtained which is to be discussed in the following section.

For simplicity and without loss of generality, we focus on the asymmetrical cavity with $\kappa_1 < \kappa_2$ to discuss the phenomenon of NUCPB. In this case, UCPB in asymmetrical cavity for the backward case can be easily obtained by alternating κ_1 with κ_2. We will in detail show the manipulation of controllable collective UCPB and NUCPB in the following section by taking or not taking the atom–atom interaction into account.

3. Manipulation of UCPB and NUCPB

3.1. Without atom–atom interaction

The atom–atom interaction makes atoms to excite each other by dipole–dipole coupling. From the energy level diagram in the collective picture, atom–atom interaction pushes down the state $|-,n\rangle$ while pulls up $|+,n\rangle$ a shift of G. Such push-and-pull effect of energy level can be used to manipulate UCPB. However, dipole–dipole coupling only occurs when two atoms are cold and close enough, and can be ignored in most common cases. Therefore, we first discuss the phenomena of UCPB and NUCPB in the absence of atom–atom interaction by setting $G = 0$.

After solving $D_3 = 0$, we can get $\eta^2 - g^2 - \Delta_{\mathrm{a}}\Delta_{\mathrm{ac}} = 0$. Letting the real and imaginary parts equal to zeros, two restrictions for producing of UCPB can be obtained mathematically, which is exactly the same to those in single-atom case.[42] The first restriction is the frequency condition

$$(\gamma + \kappa)\,\delta_{\mathrm{a}} + \gamma\delta_{\mathrm{ac}} = 0. \quad (9)$$

Here, we rewrite $\delta_{\mathrm{ac}} = \delta_{\mathrm{a}} + \delta_{\mathrm{c}}$. It shows that the detunings (δ_{a}, δ_{c}) and decay rates (γ, κ) are combined together to match

the restriction in cavity-driven case, which is different to that in atoms-driven case.[28] However, in the resonant case with $\delta_a = \delta_c = 0$, the frequency restriction is always matched naturally.

The second one is the intensity restriction,

$$n_{in} = \frac{1}{\kappa_1}\left(g^2 + \delta_a\delta_{ac} - \frac{\gamma(\gamma+\kappa)}{4}\right). \quad (10)$$

It indicates that the optimal atom–cavity coupling strength to get the fully antibunching output light relies on the incident direction,

$$g_{opt-i} = \sqrt{\kappa_i n_{in} + \gamma(\gamma+\kappa)/4 - \delta_a\delta_{ac}}, \quad (i = 1,2). \quad (11)$$

In the asymmetrical cavity, the optimal atom–cavity coupling strength shall be split into two values according to incident direction, i.e., g_{opt-1} for the forward case and g_{opt-2} for the backward case, fulfilling $g_{opt-1} < g_{opt-2}$ as we set $\kappa_1 < \kappa_2$.

From now on, we normalize all the parameters by setting $\kappa \equiv 1$ and $\kappa_{loss} = 0.02$ for simplicity and set the asymmetrical cavity with $\kappa_1 = 0.36$ and $\kappa_2 = 1.60$. In order to show UCPB in asymmetrical cavity intuitively, we plot the functions of $g^{(2)}(0)$ as a function of atom–cavity coupling strength g with respect to one-atom and two-atom cases in both forward and backward directions, as shown in Fig. 2(a). We focus on the resonant case with $\delta_a = \delta_c = 0$ to match the frequency restriction naturally, $\gamma = 0.1$ as well as $n_{in} = 0.04$ in present numerical simulation.

As expected, optical atom–cavity coupling strengths $g_{opt-1} \approx 0.2047$ and $g_{opt-2} \approx 0.3025$ separate from each other when light incidents on different walls in both one-atom and two-atom cases. In the asymmetrical cavity, spatial asymmetry breaking opens a new access to control UCPB by asymmetric cavity-loss rates.

It clearly shows that controllable UCPB in asymmetrical cavity opens a window to perform NUCPB, where the output light for the forward direction is bunching while it is antibunching for the backward case, i.e., $g_1^{(2)}(0) > 1$ and $g_2^{(2)}(0) < 1$. Here, we rewrite $g_1^{(2)}(0)$ and $g_2^{(2)}(0)$ as $g^{(2)}(0)$ for the forward and backward cases, respectively. Due to the splitting of g_{opt} in asymmetrical cavity, the curves of $g_1^{(2)}(0)$ and $g_2^{(2)}(0)$ are pushed away, and it leads to the normal NUCPB (fulfilling $g_1^{(2)}(0) > 1$ and $g_2^{(2)}(0) < 1$) in proper regime finally, where is shown by the gray rectangle in Fig. 2(a).

Controllable UCPB also makes it feasible to produce giant NUCPB (fulfilling $g_1^{(2)}(0) > 1$ and $g_2^{(2)}(0) \approx 0$). In present numerical simulation, the separation between g_{opt-1} and g_{opt-2} is far away enough to push $g_2^{(2)}(0)$ tremendously to produce fully antibunching light for the backward case while the output light is still bunching for the forward case, i.e., $g_1^{(2)}(0) > 1$ and $g_2^{(2)}(0) \approx 0$. The giant NUCPB, as specified by the yellow dotted line in Fig. 2(a), can produce the strongest UCPB nonreciprocity compared to the normal NUCPB.

In order to show giant NUCPB clearly, we focus on a case with $\omega_a = \omega_c$, and set $g = 0.3025$, $\gamma = 0.1$, and $n_{in} = 0.04$. We plot $g^{(2)}(0)$ as functions of atom–light detuning δ_a in both forward and backward cases, as shown in Fig. 2(b). The curves of $g_1^{(2)}(0)$ and $g_2^{(2)}(0)$ are deviated apparently from each other when $\delta_a = \delta_c = 0$, which is clearly shown a giant NUCPB occurs in the resonant case.

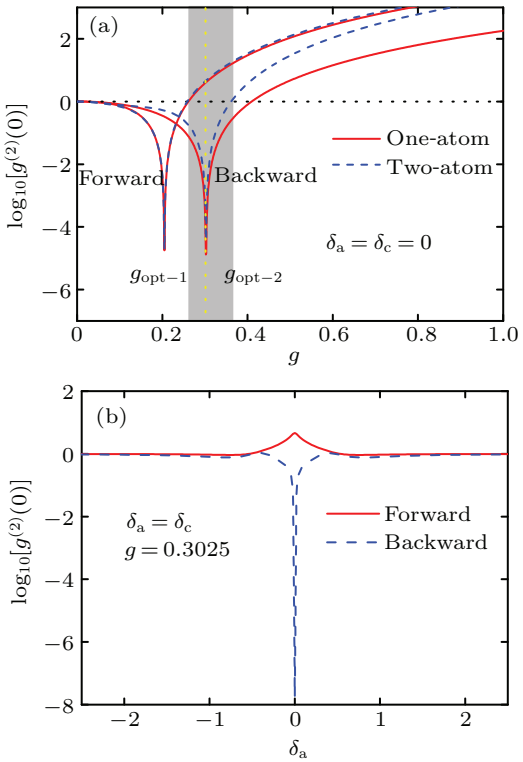


Fig. 2. UCPB and NUCPB in asymmetrical cavity without atom–atom interaction. In panel (a), the red solid curves are $g^{(2)}(0)$ for one-atom case while the blue dashed ones are for two-atom case with $\delta_a = \delta_c = 0$. Operating regime for normal NUCPB is covered by the gray rectangle while the yellow dotted line presents a giant NUCPB. Panel (b) shows $g^{(2)}(0)$ for both forward and backward incident directions in two-atom case by fixed $\delta_a = \delta_c$ and $g = 0.3025$. In both panels, the total cavity-loss rate is fixed and normalized as unit, the asymmetrical cavity is $\kappa_1 = 0.36$ and $\kappa_2 = 1.60$, and the other parameters are $\kappa_{loss} = 0.02$, $\gamma = 0.1$ and $n_{in} = 0.04$.

Compared the results in both two-atom and one-atom cases, two trapped non-interaction atoms do not harm or improve noteworthily the effects of UCPB and NUCPB as the restrictions for UCPB in both cases change nothing. It indicates that one can using two non-interaction atoms to replace a single atom in generating controllable UCPB and NUCPB.

3.2. With dipole–dipole interaction

From now on, we discuss the influence of atom–atom interaction on UCPB and NUCPB. As dipole–dipole interacts weakly in most cases, we focus our discussing on weak atom–atom interaction. After a similar process as performed above, we can get $\eta^2 - \left(2 - \frac{\Delta_{a+}}{\Delta_a}\right)g^2 - \Delta_{a+}\Delta_{ac+} = 0$. Letting the real

and imaginary parts equal to zeros, one can get restrictions for UCPB. The first restriction is the optimal atom–atom interaction condition

$$G = f_1 \cdot \left(\delta_{ac+} + \frac{\gamma+\kappa}{\gamma} \delta_{a+} \right), \tag{12}$$

where $f_1 = \left(\delta_a^2 + \gamma^2/4\right)/g^2$ and $\delta_{\alpha+} = \delta_\alpha + G$ $(\alpha = a, ac)$. When $G = 0$, the condition degenerates to $\delta_{ac} + \frac{\gamma+\kappa}{\gamma}\delta_a = 0$, which is discussed in the part A of Section 3.

The second one is a new optimal intensity restriction

$$\eta^2 = f_2 \cdot g^2 + \delta_{a+}\delta_{ac+} - \frac{\gamma(\gamma+\kappa)}{4}, \tag{13}$$

where $f_2 = \left(\delta_a \delta_{a-} + \gamma^2/4\right) / \left(\delta_a^2 + \gamma^2/4\right)$ and $\delta_{a-} = \delta_a - G$. When $G = 0$, it is easy to verify that the condition degenerates to the optimal intensity restriction discussed in the part A of Section 3.

Compared the UCPB restrictions with and without dipole–dipole interaction, the later ones are much complex and rigorous to match simultaneously since dipole–dipole interaction disturbs the quantum interfering pathways by the push-and-pull effect.

In order to show the influence of atom–atom interaction on UCPB clearly, we plot $g^{(2)}(0)$ against detunings δ_a and δ_c in Figs. 3(a) and 3(b). As a smaller γ is beneficial to produce UCPB in weak coupling regime, we set $\gamma = 0.1$, $g = 0.25$ and $\eta = 0.1980$ in the following numerical simulations, and set $G = 0$ in Fig. 3(a) while $G = 0.01$ in Fig. 3(b). Due to the push-and-pull effect induced by weak dipole–dipole interaction, UCPB regime is compressed more or less when $G = 0.01$, and the minimum of $g^{(2)}(0)$ is pull down a lot which indicates an improving NUCPB on some special points. NUCPB is promoted when the two complex UCPB restrictions are matched, while it may be suppressed when restrictions are mismatched. In general, a suppressed or promoted UCPB is depending on the working parameters.

By setting $\delta_a = \delta_c$, we plot $g^{(2)}(0)$ against G and δ_a in Fig. 3(c), as well as $g^{(2)}(0)$ against G and g in Fig. 3(d). It shows that only in a very narrow region can exist strong UCPB as G should fulfill the optimal atom–atom interaction condition and it should be rather weak. Thus we will fix $G = 0.01\gamma$ and 0.1γ in the following discussing of strong UCPB. Furthermore, the strongest UCPB effect is no longer in the resonant case due to the push-and-pull effect induced by weak dipole–dipole interaction now.

In order to show the manipulation of NUCPB, we plot the functions of $g^{(2)}(0)$ versus g with respect to different weak G in both forward and backward directions, as shown in Figs. 4(a) and 4(b). As predicted, the forward and backward correlation functions ($g_1^{(2)}(0)$ and $g_2^{(2)}(0)$) are separated from each other due to the splitting of optimal atom–cavity coupling strength (g_{opt-1} and g_{opt-2}) in asymmetrical cavity and that leads to a giant NUCPB.

Compared with the case of $G = 0$, the minima of $g_1^{(2)}(0)$ and $g_2^{(2)}(0)$ for $G = 0.01\gamma$ are changed more or less, while they are lifted up a lot for $G = 0.1\gamma$ in the case of $\delta_a = \delta_c = 0$, and reduced down a lot in the case of $\delta_a = -0.0192$ and $\delta_c = -0.1824$. Therefore, Fig. 4(a) shows a suppressed NUCPB, while Fig. 4(b) is a promoted NUCPB induced by weak atom–atom interaction. It indicates that whether the weak atom–atom interaction is harmful or beneficial to giant NUCPB is depending on the working parameters. Only when the two complex UCPB restrictions are matched can the NUCPB be promoted.

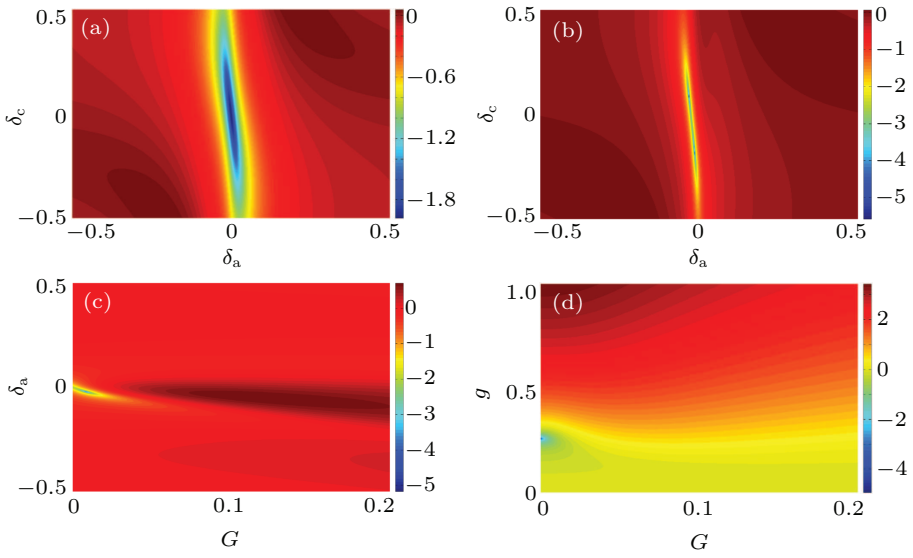


Fig. 3. Controllable UCPB with atom–atom interaction. Panels (a) and (b) are $g^{(2)}(0)$ against atom and cavity detunings for $G = 0$ and $G = 0.01$. Panel (c) is $g^{(2)}(0)$ against G and δ_a. Panel (d) is $g^{(2)}(0)$ against G and g. We set $g = 0.25$ in panels (a)–(c), $\delta_c = \delta_a$ in panels (c) and (d). In all panels, we fix $\kappa = 1$, $\kappa_{loss} = 0.02$, $\gamma = 0.1$ and $\eta = 0.1980$.

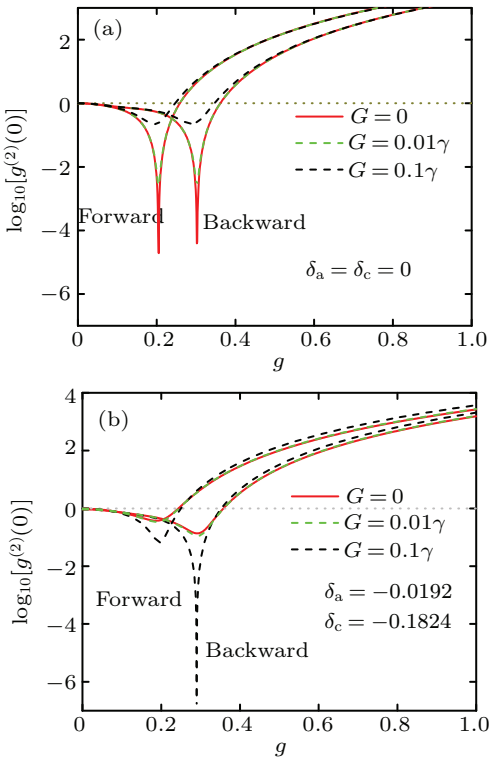


Fig. 4. Manipulation of NUCPB in asymmetrical cavity with atom–atom interaction. The red solid curves are $g^{(2)}(0)$ for $G=0$ while the green and black dashed ones are for $G=0.01\gamma$ and 0.1γ. Panel (a) is a suppressed NUCPB for $\delta_a=\delta_c=0$ and $n_{in}=0.04$ while panel (b) is a promoted NUCPB for $\delta_a=-0.0192$ and $\delta_c=-0.1824$ and $n_{in}=0.04$. The other parameters are same as those used in Fig. 2(a).

Compared with previous works of the NUCPB within the rotating optomechanical systems,[31–33] our model is all-optical without any mechanical rotation, and provides a method to manipulate UCPB by controlling atom–atom interaction. Using the existing magneto-optical trapping technology, cold atoms can be captured and moved into the optical microcavity. Therefore, it is feasible to carry out our prediction under careful designing. To our surprise, the experimental demonstration of NUCPB may has been carried out partially in atoms–cavity coupling system while the parameters are imperfect to produce giant quantum nonreciprocity.[43]

4. Conclusion

In conclusion, we have proposed a cavity-driven QED model combined an asymmetrical Fabry–Perot cavity and two identical TLAs to generate controllable UCPB and NUCPB. In the case of atom–atom direct interaction absence, the frequency and intensity restrictions of UCPB can be specified, which are identical to the restrictions of UCPB when single atom embedded. Giant NUCPB exists due to the splitting of optimal atom–cavity coupling strength in proper parameters regime. However, when a weak atom–atom interaction disturbing the quantum interference pathways is taken into account, two restrictions of UCPB are modified complexly, which are rigorous to be matched simultaneously. It makes the region of UCPB to be compressed more or less while the effect of UCPB can be improved as a smaller minimum of $g^{(2)}(0)$ may be presented. We also examine the influence of NUCPB by weak atom–atom interaction and giant NUCPB occurs when atom–atom interaction is weak enough. In general, whether the giant NUCPB is suppressed or promoted depends on the working parameters.

Acknowledgements

Project supported by the National Natural Science Foundation of China (Grants Nos. 12164022, 11864018, and 12174288) and the Fundamental Research Funds for the Provincial Universities of Zhejiang Province, China (Grant No. GK199900299012-015).

References

[1] Leoński W and Miranowicz A 2004 *J. Opt. B* **6** S37
[2] Birnbaum K M, Boca A, Miller R, Boozer A D, Northup T E and Kimble H J 2005 *Nature* **436** 87
[3] Zou F, Zhang X Y, Xu X W, Huang J F and Liao J Q 2020 *Phys. Rev. A* **102** 053710
[4] Zhou Y H, Zhang X Y, Wu Q C, Ye B L, Zhang Z Q, Zou D D, Shen H Z and Yang C P 2020 *Phys. Rev. A* **102** 033713
[5] Shen S, Li J and Wu Y 2020 *Phys. Rev. A* **101** 023805
[6] Liang X, Duan Z, Guo Q, Guan S, Xie M and Liu C 2020 *Phys. Rev. A* **102** 053713
[7] Kyriienko O, Krizhanovskii D N and Shelykh I A 2020 *Phys. Rev. Lett.* **125** 197402
[8] Rabl P 2011 *Phys. Rev. Lett.* **107** 063601
[9] Hoffman A J, Srinivasan S J, Schmidt S, Spietz L, Aumentado J, Türeci H E and Houck A A 2011 *Phys. Rev. Lett.* **107** 053602
[10] Imamoğlu A, Schmidt H, Woods G and Deutsch M 1997 *Phys. Rev. Lett.* **79** 1467
[11] Dayan B, Parkins A S, Aoki T, Ostby E P, Vahala K J and Kimble H J 2008 *Science* **319** 1062
[12] Faraon A, Fushman I, Englund D, Stoltz N, Petroff P and Vučković J 2008 *Nat. Phys.* **4** 859
[13] Reinhard A, Volz T, Winger M, Badolato A, Hennessy K J, Hu E L and Imamoğlu A 2012 *Nat. Photon.* **6** 93
[14] Lang C, Bozyigit D, Eichler C, Steffen L, Fink J M, Abdumalikov A A, Baur M, Filipp S, da Silva M P, Blais A and Wallraff A 2011 *Phys. Rev. Lett.* **106** 243601
[15] Liew T C H and Savona V 2010 *Phys. Rev. Lett.* **104** 183601
[16] Flayac H and Savona V 2017 *Phys. Rev. A* **96** 053810
[17] Flayac H and Savona V 2013 *Phys. Rev. A* **88** 033836
[18] Wang H, Gu X, Liu Y X, Miranowicz A and Nori F 2015 *Phys. Rev. A* **92** 033806
[19] Sarma B and Sarma A K 2018 *Phys. Rev. A* **98** 013826
[20] Gao Y P, Liu X F, Wang T J, Cao C and Wang C 2019 *Phys. Rev. A* **100** 043831
[21] Sarma B and Sarma A K 2017 *Phys. Rev. A* **96** 053827
[22] Zhao D 2018 *Phys. Rev. A* **98** 033834
[23] Vaneph C, Morvan A, Aiello G, Féchant M, Aprili M, Gabelli J and Estève J 2018 *Phys. Rev. Lett.* **121** 043602
[24] Snijders H J, Frey J A, Norman J, Flayac H, Savona V, Gossard A C, Bowers J E, van Exter M P, Bouwmeester D and Löffler W 2018 *Phys. Rev. Lett.* **121** 043601
[25] Cidrim A, do Espirito Santo T S, Schachenmayer J, Kaiser R and Bachelard R 2020 *Phys. Rev. Lett.* **125** 073601
[26] Williamson L A, Borgh M O and Ruostekoski J 2020 *Phys. Rev. Lett.* **125** 073602
[27] Zhu C J, Yang Y P and Agarwal G S 2017 *Phys. Rev. A* **95** 063842
[28] Hou K, Zhu C J, Yang Y P and Agarwal G S 2019 *Phys. Rev. A* **100** 063817
[29] Lin J Z, Hou K, Zhu C J and Yang Y P 2019 *Phys. Rev. A* **99** 053850
[30] Li B, Huang R, Xu X, Miranowicz A and Jing H 2019 *Photonics Res.* **7** 630

[31] Huang R, Miranowicz A, Liao J Q, Nori F and Jing H 2018 *Phys. Rev. Lett.* **121** 153601
[32] Wang K, Wu Q, Yu Y F and Zhang Z M 2019 *Phys. Rev. A* **100** 053832
[33] Shen H Z, Wang Q, Wang J and Yi X X 2020 *Phys. Rev. A* **101** 013826
[34] Jiao Y F, Zhang S D, Zhang Y L, Miranowicz A, Kuang L M and Jing H 2020 *Phys. Rev. Lett.* **125** 143605
[35] Bamba M, Imamoğlu A, Carusotto I and Ciuti C 2011 *Phys. Rev. A* **83** 021802
[36] Xu X W, Li Y, Li B, Jing H and Chen A X 2020 *Phys. Rev. Appl.* **13** 044070
[37] Xu X, Zhao Y, Wang H, Jing H and Chen A 2020 *Photonics Res.* **8** 143
[38] Jalas D, Petrov A, Eich M, Freude W, Fan S, Yu Z, Baets R, Popovic M, Melloni A, Joannopoulos J D, Vanwolleghem M, Doerr C R and Renner H 2013 *Nat. Photonics* **7** 579
[39] Xia X, Xu J and Yang Y 2014 *J. Opt. Soc. Am. B* **31** 2175
[40] Yang P, Xia X, He H, Li S, Han X, Zhang P, Li G, Zhang P, Xu J, Yang Y and Zhang T 2019 *Phys. Rev. Lett.* **123** 233604
[41] Xia X, Xu J and Yang Y 2014 *Phys. Rev. A* **90** 043857
[42] Xia X, Zhang X, Xu J, Li H, Fu Z and Yang Y 2021 *Phys. Rev. A* **104** 063713
[43] Yang P, Li M, Han X, He H, Li G, Zou C L, Zhang P and Zhang T 2019 arXiv **1911** 10300v